Molecular Cell
Article

Arabidopsis Argonaute 2 Regulates Innate Immunity via miRNA393*-Mediated Silencing of a Golgi-Localized SNARE Gene, *MEMB12*

Xiaoming Zhang,[1,3,4,7] Hongwei Zhao,[1,3,4,7] Shang Gao,[1,3,4] Wei-Chi Wang,[5] Surekha Katiyar-Agarwal,[1,3,4,8] Hsien-Da Huang,[5,6] Natasha Raikhel,[2,3,4] and Hailing Jin[1,3,4,*]
[1]Department of Plant Pathology and Microbiology
[2]Department of Botany and Plant Sciences
[3]Center for Plant Cell Biology
[4]Institute for Integrative Genome Biology
University of California, Riverside, Riverside, CA 92521, USA
[5]Institute of Bioinformatics and Systems Biology
[6]Department of Biological Science and Technology
National Chiao Tung University, Hsin-Chu 300, Taiwan
[7]These authors contributed equally to this work
[8]Present address: Department of Plant Molecular Biology, University of Delhi South Campus, New Delhi 110021, India
*Correspondence: hailingj@ucr.edu
DOI 10.1016/j.molcel.2011.04.010

SUMMARY

Argonaute (AGO) proteins are critical components of RNA silencing pathways that bind small RNAs and mediate gene silencing at their target sites. We found that *Arabidopsis* AGO2 is highly induced by the bacterial pathogen *Pseudomonas syringae* pv. *tomato* (*Pst*). Further genetic analysis demonstrated that AGO2 functions in antibacterial immunity. One abundant species of AGO2-bound small RNA is miR393b*, which targets a Golgi-localized SNARE gene, *MEMB12*. *Pst* infection downregulates MEMB12 in a miR393b*-dependent manner. Loss of function of *MEMB12*, but not *SYP61*, another intracellular SNARE, leads to increased exocytosis of an antimicrobial pathogenesis-related protein, PR1. Overexpression of miR393b* resembles *memb12* mutant in resistance responses. Thus, AGO2 functions in antibacterial immunity by binding miR393b* to modulate exocytosis of antimicrobial PR proteins via MEMB12. Since miR393 also contributes to antibacterial responses, miR393*/miR393 represent an example of a miRNA*/miRNA pair that functions in immunity through two distinct AGOs: miR393* through AGO2 and miR393 through AGO1.

INTRODUCTION

Small RNA (sRNA)-mediated gene silencing has been recognized as an important regulatory mechanism in host immune responses of both plants and animals (Ding, 2010; Padmanabhan et al., 2009; Wessner et al., 2010). Plants have evolved multiple levels of immune responses, including basal defense triggered by virulent pathogens in susceptible hosts and resistance (*R*) gene-mediated resistance activated by avirulent pathogens in resistant hosts. Conserved microbial- or pathogen-associated molecular patterns (MAMPs or PAMPs) are recognized by host pattern recognition receptors and activate PAMP-triggered immunity (PTI), whereas pathogen-derived effector proteins, which can attenuate PTI, are recognized by host R proteins and trigger effector-triggered immunity (ETI) (Chisholm et al., 2006; Jones and Dangl, 2006). In *Arabidopsis*, microRNA393 (miR393) negatively regulates auxin signaling pathways and contributes to PTI (Navarro et al., 2006). Endogenous small interfering RNAs (siRNAs), nat-siRNAATGB2 and AtIsiRNA-1, are induced by the bacterial pathogen *Pseudomonas syringae* pv. *tomato* (*Pst*) DC3000 carrying an effector gene, *avrRpt2*; these siRNAs play an important role in ETI by targeting negative regulators of the cognate *R* gene *RPS2* signaling pathway (Katiyar-Agarwal et al., 2006, 2007).

sRNAs are loaded into Argonaute proteins (AGOs) and silence targets with complementary sequences. Many eukaryotes have evolved functionally diversified AGOs that regulate many cellular processes (Hutvagner and Simard, 2008; Mallory and Vaucheret, 2010). Specific AGOs from *Drosophila*, *Arabidopsis*, *C. elegans*, and *Cryphonectria parasitica* are essential for antiviral defenses by binding viral sRNAs and silencing viral genomes (Ding, 2010; Harvey et al., 2011). However, function of AGOs in antibacterial immunity is less clear. *Arabidopsis* encodes ten AGOs (Vaucheret, 2008). AGO1 is primarily associated with miRNAs and mainly regulates plant development and stress adaptations (Mallory and Vaucheret, 2010). AGO1 also contributes to PTI through several stress-related miRNAs (Li et al., 2010b). AGO7 mainly binds miR390 and triggers the generation of *trans*-acting siRNAs (Montgomery et al., 2008); it is required for the accumulation of AtIsiRNA-1 and contributes to ETI (Katiyar-Agarwal et al., 2007; Li et al., 2010b). AGO4, AGO6, and AGO9 predominantly bind heterochromatic siRNAs from different loci and function in RNA-directed DNA methylation (RdDM) (Havecker et al., 2010; Mallory and Vaucheret, 2010). AGO4 has been linked to antibacterial defense (Agorio and Vera, 2007). Whether these

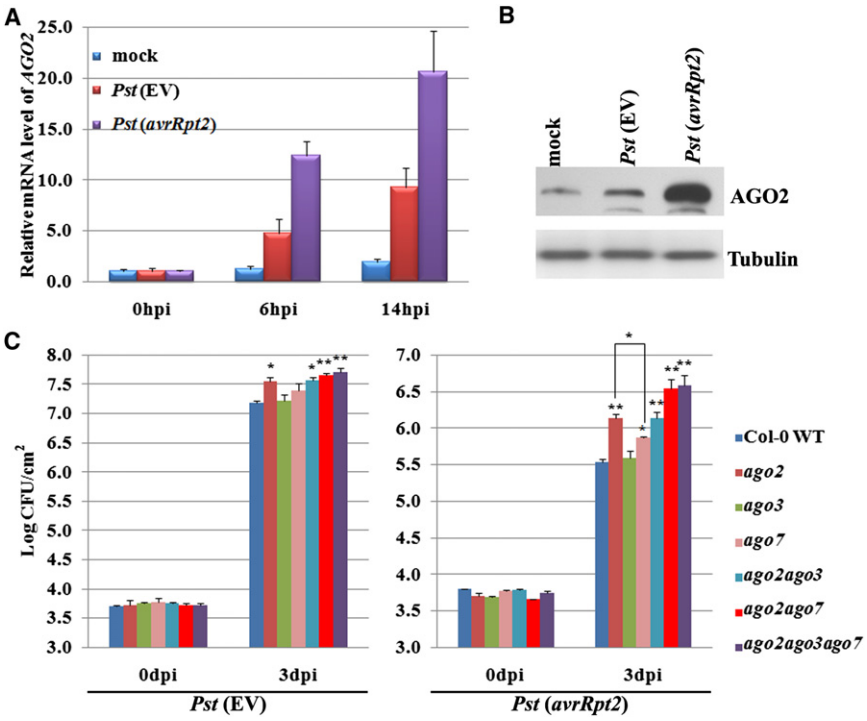

Figure 1. *AGO2* Is Highly Induced by *Pst*, and Mutation in *AGO2* Attenuates Plant Resistance to Both Virulent and Avirulent Strains of *Pst*

(A) *AGO2* transcript was highly induced by *Pst* (EV) and *Pst* (*avrRpt2*). Sample leaves were collected at 6 and 14 hpi. Relative transcript levels were measured by real-time RT-PCR. *Actin2* was used as an internal control. Standard deviations were calculated from three technical replicates. Similar results were obtained from three biological replicates.

(B) Western blot analysis of AGO2 in response to *Pst* (EV) and *Pst* (*avrRpt2*) infection. The samples were collected at 14 hpi and AGO2 was detected by a peptide antibody (Harvey et al., 2011). Tubulin was used as a control. Similar results were observed from two replicates.

(C) *ago2* single, double, and triple mutants were more susceptible to *Pst* (EV) and *Pst* (*avrRpt2*) than WT plants. Four-week-old plants were infiltrated with *Pst* (EV) and *Pst* (*avrRpt2*) (5×10^5 cfu/ml). Error bars represent standard deviation of six leaf discs. Student's t test was performed to determine the significant differences between mutants and WT plants. Asterisks "*" and "**" indicate statistically significant differences at a p value of <0.05 and <0.01, respectively. Similar results were obtained from three biological replicates. See Figure S1 for expression levels of other *Arabidopsis* AGOs, characterization of *ago2* mutants, and miR403 expression analysis.

activities of AGO4 involve sRNAs or RdDM, however, is unknown, because none of the other factors involved in the RdDM pathway has effects on antibacterial immunity (Agorio and Vera, 2007).

To understand the differentiated function of *Arabidopsis* AGOs in plant immunity, we examined the expression of all the *AGO* genes in response to bacterial infection. We show that *AGO2* is highly induced by *Pst* and that *AGO2* mutation attenuates antibacterial immunity. Profiling of AGO2-bound sRNAs by high-throughput sequencing revealed that one of the most abundant sRNAs is miR393b*, which targets a gene encoding a Golgi-localized, SDS-resistant, soluble N-ethylmaleimide-sensitive factor attachment protein receptor (SNARE) protein, MEMB12. Mutation in *MEMB12* but not *SYP61*, another intracellular SNARE gene, leads to increased exocytosis of the antimicrobial pathogenesis-related protein PR1. miR393 is known to contribute to PTI. Here, we show that miR393* also contributes to immunity, mainly ETI, by modulating secretion of PR1. Thus, we provide an example of a functional pair of miRNA* and miRNA, each of which targets different regulators in host innate immunity through two distinct AGOs: miR393* through AGO2 and miR393 through AGO1.

RESULTS

Arabidopsis AGO2 Is Highly Induced by Bacterial Infection and Plays an Important Role in Innate Immune Responses

To further our understanding of the differentiated function of AGOs in antibacterial immunity, we first examined the expression of all *AGO* genes in response to the infection of *Pst* DC3000. Transcripts of *AGO2*, but no other *AGOs*, were induced by the virulent strain of *Pst* carrying an empty vector (EV). This induction was even more pronounced in response to an avirulent strain, *Pst* (*avrRpt2*), at 6 and 14 hr postinoculation (hpi) (Figures 1A and S1A). Western blot analysis confirmed that AGO2 protein level was also highly induced by both *Pst* (EV) and *Pst* (*avrRpt2*) (Figure 1B).

To determine whether AGO2 regulates immune responses against bacterial infection, we carried out a bacterial growth assay on a loss-of-function mutant, *ago2-1* (Lobbes et al., 2006). *ago2-1* displayed enhanced susceptibility to *Pst* (*avrRpt2*) and supported 5- to 6-fold more bacterial growth than wild-type (WT) Col-0 at 3 days postinoculation (dpi) (Figure 1C). It also consistently showed moderately enhanced susceptibility to *Pst* (EV), permitting 3- to 4-fold more bacterial growth than WT (Figure 1C). Of the ten *Arabidopsis* AGOs, AGO2 is closely related to AGO3 and AGO7. Consistent with previous reports (Katiyar-Agarwal et al., 2007; Li et al., 2010b), an *ago7* mutant (*zip-1* [Hunter et al., 2003]) was more susceptible to *Pst* (*avrRpt2*) but not to *Pst* (EV) (Figure 1C). However, the effect of *ago7* was weaker than that of *ago2-1* ($p < 0.05$). No alteration in bacteria growth was observed in *ago3-1* (Figure 1C) (Lobbes et al., 2006).

To test whether *AGO2*, *AGO3*, and *AGO7* are partially redundant, double and triple mutants were generated. *ago2ago7* was generated by crossing the relevant single mutants; *ago2ago3* and *ago2ago3ago7* were obtained by generating transgenic *AGO3* RNAi lines in the background of *ago2-1* and *ago2ago7*, respectively. Since *AGO2* (At1g31280) and *AGO3* (At1g31290)

Table 1. miRNA*s Are Highly Enriched in the AGO2-IP Fraction

	AGO2-IP		AGO1-IP		Total sRNA without IP	
	Mock	*Pst* (*avrRpt2*)	Mock	*Pst* (*avrRpt2*)	Mock	*Pst* (*avrRpt2*)
miR393b*	2621.9	4546.6	0.3	24.4	36.6	89.6
miR393	0.4	0.5	358.1	156.6	11.7	75.3
miR165a*	7943.4	15529.2	1.0	0.9	146.2	531.5
miR165a	0.3	6.3	30890.4	23823.2	300.3	177.2
miR396b*	1196.9	2864.6	188.2	214.6	76.4	10.2
miR396b	26.3	28.4	4121.9	6173.0	214.8	42.8
miR472*	508.7	1273.7	28.1	36.4	127.3	79.4
miR472	0.9	2.0	246.9	61.5	2.6	5.1

Normalized miRNA* and miRNA (reads/mgs) from each sRNA library are listed. Total sRNAs without IP from our previous data set (Chellappan et al., 2010; Zhang et al., 2010, 2011) are included as controls. AGO2-associated miRNA*s with more than 1000 reads/mgs are shown. See Table S1 for the full list of miRNA and miRNA* from the AGO-IP deep sequencing data set.

are closely linked on chromosome 1, it is impossible to obtain an *ago2ago3* double mutant by crossing the single mutants. The transgenic *AGO3* RNAi lines with the lowest *AGO3* expression level were selected for functional analysis (Figures S1B and S1C). *ago2ago7* and *ago2ago3ago7* behaved very similarly and showed more susceptibility to *Pst* (*avrRpt2*) than *ago2* or *ago7* single mutants, allowing 9- to 10-fold more bacterial growth than WT plants (Figure 1C), confirming that both AGO2 and AGO7 contribute to ETI. Bacterial growth in *ago2ago3* was similar to that in *ago2*, which confirmed that *ago3* has little effect on the resistance (Figure 1C). *Pst* (EV) grew to a similar level in the *ago2* single, double, and triple mutants, suggesting that only AGO2 is involved in basal defense. The precise definition of basal defense is PTI plus weak ETI, minus effector-triggered susceptibility (Jones and Dangl, 2006). To determine whether AGO2 plays a role in PTI, we performed flg22-mediated protection assay (Zipfel et al., 2004). Inhibition of *Pst* (EV) growth by flg22 pretreatment was observed in both *ago2* and WT plants (Figure S1D). Flg22 treatment also caused growth inhibition of the *ago2* mutant to a similar level as with WT (Figure S1E). Furthermore, we still detected clear induction of *AGO2* in response to *Pst* (EV) infection in *bak1* mutant (Figure S1F). BAK1 is a common signaling component in PTI. These data suggest that AGO2 may play a minor role, if any, in PTI.

The bacterial effector avrRpt2 is recognized by its cognate R protein RPS2 in Col-0 and triggers local cell death, which is referred to as the hypersensitive response (HR). Under the conditions we used, visible HR occurred at 15 hpi in WT plants, but not in *ago2ago7* and *ago2ago3ago7* (Figure S1G). A delayed HR (at 17–18 hpi) to *Pst* (*avrRpt2*) was observed in *ago2ago7* and *ago2ago3ago7*. Taken together, our results indicate that AGO2 plays an important role in plant innate immunity, especially in ETI against bacterial pathogens.

miR393b* Is Highly Enriched in AGO2

We hypothesized that, as a critical component of the RNAi pathway, AGO2 regulates plant immunity through the action of its bound sRNAs. Therefore, we used Illumina deep sequencing to analyze the AGO2-associated sRNA population after *Pst* (*avrRpt2*) and mock treatments using a transgenic *AGO2::3HA-AGO2* line (Montgomery et al., 2008). The data set was deposited into NCBI (GSE26161). AGO1-associated sRNA libraries prepared under the same conditions were used as controls. Consistent with previous reports (Mi et al., 2008; Montgomery et al., 2008), AGO2-associated sRNAs were primarily 21 nt in length and had a bias for reads with the 5′-terminal A, whereas AGO1-bound sRNAs were mainly 21 nt miRNAs with 5′-terminal U. Strikingly, among the most abundant AGO2-bound sRNAs (Tables 1 and S1), several miRNA*s, including miR165a*, miR393b*, miR396b*, and miR472*, had more than 1000 reads per million genome-matched sequences (mgs) (Table 1). miRNA*s are sRNA species that pair with corresponding miRNAs within the hairpin structure of the miRNA precursors and are processed into miRNA:miRNA* duplexes by Dicer or Dicer-like proteins. They were often considered as nonfunctional by-products because they are quickly degraded and are much less abundant than their corresponding miRNAs. However, we observed significant enrichment of several of these miRNA*s in the AGO2-immunoprecipitated (IP) fraction, suggesting that they may be biologically functional.

One of the most abundant miRNA*s that associated with AGO2 was miR393b*, which had more than 4500 reads/mgs in the AGO2-IP fraction after *Pst* (*avrRpt2*) treatment, but had only 24 reads/mgs in the AGO1-IP faction (Table 1). Interestingly, its corresponding miR393 was only present in the AGO1-IP but not the AGO2-IP fraction (Table 1). miR393 has been shown to contribute to PTI by silencing auxin receptors (Navarro et al., 2006). Therefore, we were very interested in testing whether miR393b* has a regulatory role like its miRNA partner. Mature miR393a and miR393b have the same sequence, but miR393a* and miR393b* differ in one nucleotide, and miR393b* is much more abundant than miR393a* (4546 versus 25 reads/mgs in the *Pst* (*avrRpt2*)-treated AGO2-IP libraries) (Table S1). To confirm that miR393b* and miR393 were incorporated into two different AGO proteins (AGO2 and AGO1, respectively), we performed sRNA northern blot analysis using total RNA from *ago* mutants and sRNA fractions from the AGO-IPs. Expression of miR393b* was almost abolished in *ago2-1*, while its corresponding miR393 was reduced in *ago1-27*, a relatively weak allele (Figure 2A) (Morel et al., 2002). miR393b* was detected only in AGO2- but not AGO1-IP fractions, whereas miR393 appeared only in AGO1- but not AGO2-IP fractions

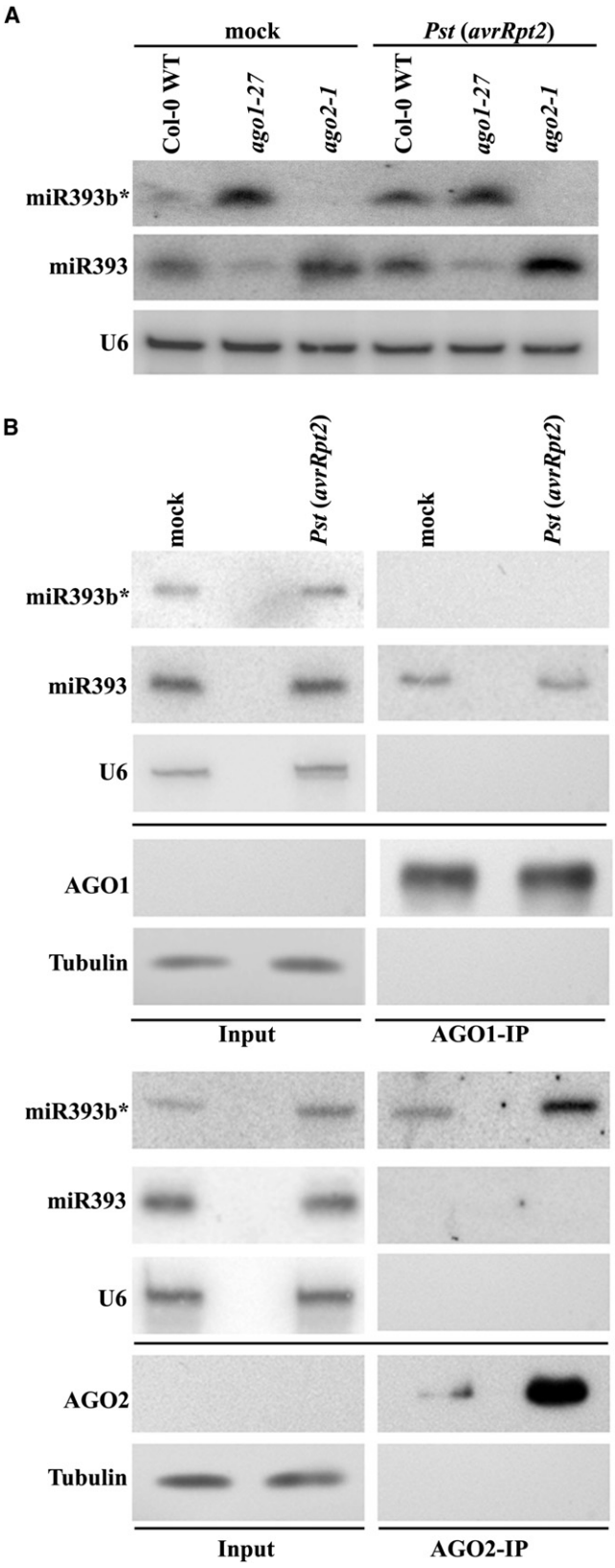

Figure 2. miR393b* Is Associated with AGO2, Whereas miR393 Is Associated with AGO1

(A and B) Accumulation of miRNA393b* and miRNA393 in Col-0 WT, *ago1-27*, and *ago2-1* mutants (A) or in AGO1-IP and AGO2-IP (B) was detected by miRNA393b* and miRNA393 probes. Mock- or *Pst* (*avrRpt2*)-treated leaves (*AGO2::3HA-AGO2*) were collected at 12 hpi. Forty micrograms of total RNA was used for each genotype in (A). For RNA IP, cell lysate from 0.15 g of tissue was incubated with AGO1 antibody or HA antibody for pulling down AGO1 and AGO2 fraction, respectively (see Experimental Procedures for details). Total RNA (without IP procedures) equivalents to 0.03 g of plant tissue were loaded as the input control. The IP efficiency was examined by detecting AGO1 and AGO proteins in the IP fractions (from 0.15 g plant tissue) using AGO1 antibody and HA antibody, respectively. Thirty microliters of original homogenized tissue (corresponding to 0.005 g) was loaded in the input panels. Tubulin was used as a loading control. Similar results were obtained in three biological replicates. See Table S1 for the rest of miRNA*s and miRNAs from the AGO pull-down sequencing data set.

(Figure 2B). These results confirmed that miR393b* and miR393 were bound to distinct AGOs. The level of miR393b* associated with AGO2 was significantly increased after *Pst* (*avrRpt2*) infection (Figure 2B), most likely due to the induction of AGO2. These results strongly suggest that miR393b* is functional.

miR393b* Targets *MEMB12* Encoding a SNARE Protein

Recent studies in animals suggested that some miRNA*s may have regulatory roles (Ghildiyal et al., 2010; Guo and Lu, 2010; Okamura et al., 2008). However, in vivo functional analyses of these miRNA*s have not been reported. We proposed that miR393b* regulates plant immunity by targeting genes involved in plant defense responses. Therefore, we predicted potential targets of miR393b* (Table S2). Three of the putative targets, At5g50440, At4g19490, and At3g09530, have predicted roles in protein trafficking and secretion. At5g50440 encodes MEMB12, a Golgi-localized SNARE protein (Uemura et al., 2004), but its biological function has not been determined. At4g19490 encodes a Golgi/post-Golgi compartment-localized protein, VPS54, which is the homolog of a subunit of yeast Golgi-associated retrograde protein (GARP)/Vps Fifty Three (VFT) complex involved in retrograde transport from the vacuolar/late endosome compartment to the Golgi apparatus (Conibear and Stevens, 2000; Guermonprez et al., 2008). At3g09530 encodes EXO70H3, which belongs to the large EXO70 gene family and is a subunit of the exocyst complex predicted to be responsible for exocytosis (Li et al., 2010a). The expression of *EXO70H3* in leaves is below the detection limit (Li et al., 2010a). Several plasma membrane (PM)-associated proteins involved in cell surface trafficking have been shown to be essential in plant immune responses, which indicates the importance of protein trafficking in plant defense (Bednarek et al., 2010; Collins et al., 2003; Kalde et al., 2007; Kwon et al., 2008). However, proteins responsible for intracellular vesicle transport and the early steps of protein secretion have not been identified in host immune responses. Two of the putative targets, MEMB12 and VPS54, are localized to the Golgi apparatus and have a predicted function in vesicle transport. Mutations in *VPS54* and other GARP subunits display a transmission defect through the male gametophyte and could not yield homozygous mutants (Guermonprez et al., 2008), making it

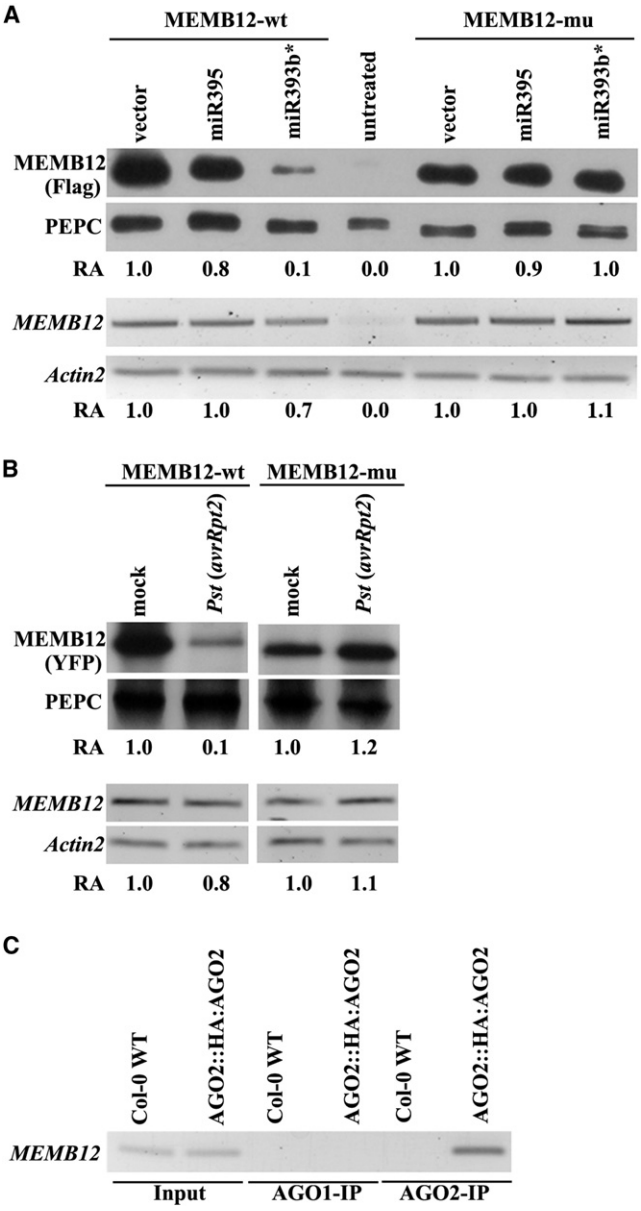

Figure 3. *MEMB12* Is a Target of miR393b*

(A) miR393b* downregulates MEMB12 in a transient coexpression assay in *N. benthamiana*. The Flag-tagged expression construct of *MEMB12-wt* or *MEMB12*-mu was coexpressed with miR393b* or miR395 in *N. benthamiana*. The protein levels (the upper panel) were detected by an anti-FLAG antibody. Phosphoenolpyruvate carboxylase (PEPC) was used as a loading control for measuring the relative abundance (RA) (shown below) using the ImageQuant software. The transcript levels of *MEMB12* from the same treatment were measured by semiquantitative RT-PCR (bottom panel). *Actin2* was used for measuring the RA (shown below). Similar results were obtained in two biological replicates.

(B) miR393b* downregulates MEMB12 in stable transgenic *Arabidopsis*. Transgenic *Arabidopsis* carrying *MEMB12-wt* and *MEMB12-mu* (*35S::YFP:MEMB12*) were generated. The protein level of MEMB12 in the selected line after mock or *Pst* (*avrRpt2*) treatment was detected by an anti-GFP antibody. The transcript level of *MEMB12* was measured as in (A). The experiments were repeated three times, and similar results were observed.

(C) *MEMB12* mRNA was coimmunoprecipitated with AGO2 but not AGO1. RNAs from input, AGO1-IP, and AGO2-IP fractions from both transgenic (*AGO2::3HA-AGO2*) and Col-0 WT plants were reverse transcribed and amplified using *MEMB12*-specific primers. The PCR bands were gel purified and confirmed by sequencing. Similar results were observed in two independent experiments. See Figure S2 for the alignment between miR393b* and *MEMB12-wt* and *MEMB12-mu*.

very difficult to test the role of VPS54 in plant defense. Therefore, in this study we focused on the characterization of MEMB12—a Golgi-localized SNARE protein—in plant immune responses.

To test experimentally whether *MEMB12* is a real target of miR393b*, we first performed *Agrobacterium*-mediated transient coexpression assays in *Nicotiana benthamiana*. A binary construct carrying the Flag-tagged *MEMB12* with the WT miR393b* target site (*MEMB12-wt*) was coexpressed with miR393b* or miR395, a miRNA that cannot target *MEMB12*. The MEMB12 protein level was downregulated by miR393b* but not miR395 (Figure 3A). This downregulation was abolished when the miR393b* target site in *MEMB12* was mutated (*MEMB12-mu*, with no amino acid change) (Figures 3A and S2). These results indicate that miR393b* is responsible for the downregulation of MEMB12. The protein level of MEMB12 was significantly reduced while its transcript level was reduced only slightly, suggesting that miR393b* silences *MEMB12* mainly by translational inhibition. We also generated transgenic *Arabidopsis* carrying *YFP-MEMB12-wt* or *YFP-MEMB12-mu* to test the regulatory role of miR393b* in vivo. MEMB12-wt protein was downregulated after *Pst* (*avrRpt2*) treatment, whereas MEMB12-mu was not (Figure 3B). The mRNA level of *MEMB12-wt* was not significantly reduced after infection of *Pst* (*avrRpt2*) (Figure 3B), consistent with the notion that miR393b* mainly mediates translational inhibition rather than mRNA degradation. If *MEMB12* is the target of miR393b*, *MEMB12* transcripts should also be associated with AGO2, which is the AGO predominantly associated with miR393b*. Indeed, *MEMB12* mRNA was enriched in the AGO2-IP fraction but was not detected in the AGO1-IP fraction (Figure 3C). These results supported that *MEMB12* is a real target of miR393b*.

Loss of Function of *MEMB12* Promotes Secretion of PR1

To test whether *MEMB12* plays a role in antibacterial defense, we isolated the *MEMB12* knockout mutant *memb12-1* (GT22391), which is a transposon-tagged line with an insertion in the first exon (Figures S3A–S3C) (Springer et al., 1995). *memb12-1* had no obvious developmental defects, but displayed enhanced resistance to both avirulent and virulent strains of *Pst*. Growth of *Pst* (*avrRpt2*) in *memb12-1* was reduced 5- to 6-fold compared with the WT control (Figure 4A). *memb12-1* also showed enhanced resistance to *Pst* (EV), although to a lesser degree (Figure 4A).

To understand the mechanism of function of *MEMB12* in innate immunity, we analyzed the localization of MEMB12 by examining the transgenic *YFP-MEMB12-wt* plants. We observed punctate structures in the cytosol (Figure S3D), which is the characteristic feature of the plant Golgi apparatus (Chatre et al., 2005; Matheson et al., 2006). This observation is in accordance with previously reported MEMB12 localization to the Golgi

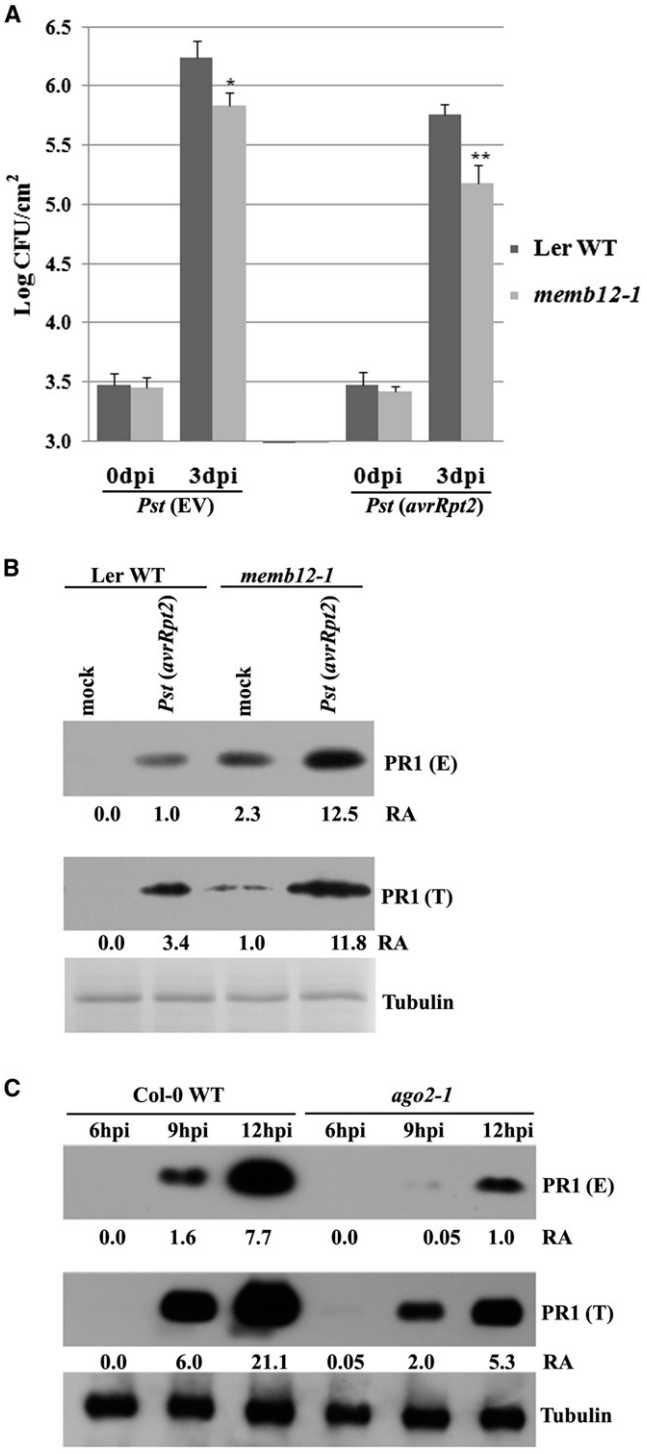

Figure 4. Mutation in *MEMB12* Leads to Enhanced Resistance to Both *Pst* (EV) and *Pst* (*avrRpt2*) and Promotes PR1 Secretion

(A) Growth of *Pst* (EV) and *Pst* (*avrRpt2*) was measured in 4-week-old *memb12-1* and corresponding Ler WT as described in Figure 1C. Error bars represent standard deviation of six leaf discs (*$p < 0.05$; **$p < 0.01$). Similar results were obtained in three biological replicates.

(B) *memb12-1* promotes PR1 secretion. The level of PR1 in total (T; whole leaf) and secreted proteins (E; intercellular wash fluid) from mock- and *Pst* (*avrRpt2*)-treated Ler WT and *memb12-1* plants was detected by western blot analysis. Equal volume of intercellular wash fluid was loaded for detecting secreted PR1. Tubulin was used as an equal loading control and RA measurement for detecting total PR1 protein. Similar results were observed from four biological repeats.

(C) Secretion of PR1 was reduced and delayed in *ago2-1* mutant plants. The total (T) and secreted (E) PR1 were compared between Col-0 WT and *ago2* plants at 6, 9, and 12 hpi of *Pst* (*avrRpt2*). Similar results were obtained from three biological repeats (Figure S3). See Figure S3 for the characterization of *memb12-1* mutant and the analysis of PR1 level in *ago2-1*.

(Geldner et al., 2009; Uemura et al., 2004). Secretion of antimicrobial proteins or small molecules is essential for effective defense against pathogens (Bednarek et al., 2010; Collins et al., 2003; Kalde et al., 2007; Kwon et al., 2008; Nomura et al., 2006). To examine whether MEMB12 suppresses defense responses by affecting protein secretion, we examined the level of one of the major secreted antimicrobial pathogenesis-related proteins—PR1—in the intercellular wash fluid of *memb12-1* before and after bacterial infection as described (Wang et al., 2005). After *Pst* (*avrRpt2*) infection, the level of intercellular secreted PR1 was more than 10-fold greater in *memb12-1* than in WT (Figure 4B), while total PR1 protein only increased by about 3- to 4-fold in *memb12-1* compared with that in WT (Figure 4B). These results indicate that the secretion of PR1 in *memb12-1* is indeed increased. Secreted PR1 also accumulated in the mock-treated *memb12-1* (Figure 4B). Furthermore, the secretion of PR1 upon *Pst* (*avrRpt2*) infection was significantly reduced and delayed in the *ago2-1* mutant (Figures 4C, S3E, and S3F), which is consistent with the result that *ago2* was more susceptible to *Pst* (*avrRpt2*) (Figure 1C).

On the contrary, mutation in the trans-Golgi network (TGN)/endosomal SNARE *SYP61* gene did not alter the secretion level of PR1 (Figure 5A) (Robert et al., 2008; Sanderfoot et al., 2001; Sanmartín et al., 2007; Zhu et al., 2002). These results suggest that intracellular SNARE MEMB12 but not SYP61 specifically controls the exocytosis of vesicles containing antimicrobial protein PR1.

To determine whether suppression of MEMB12 interferes with general protein secretion, we also examined the level of another secreted protein: SYP121, a PM-associated syntaxin required for resistance to powdery mildew fungus (Collins et al., 2003). The level of SYP121 was slightly increased in the PM factions in *memb12-1* as compared with WT plants (Figure 5B). Mutation in *MEMB12* has a much smaller effect on SYP121 secretion than on PR1 secretion, suggesting that MEMB12 is responsible for trafficking of a specific group of proteins, such as PR1.

When massive accumulation and secretion of PR proteins occur during defense responses, a coordinated upregulation of the whole protein secretory machinery is often accompanied to ensure efficient transport (Wang et al., 2005). Indeed, we detected upregulation in *memb12-1* of several secretion pathway genes that encode translocon complex Sec61 α subunit, cochaperone Calnexin 1, a Clathrin-coat assembly protein, and a Vacuolar sorting receptor VSR6; upregulation occurred even without pathogen challenges (Figure 5C), which suggests that suppression of MEMB12 leads to an upregulation of the secretory pathway for transporting certain proteins. Taken

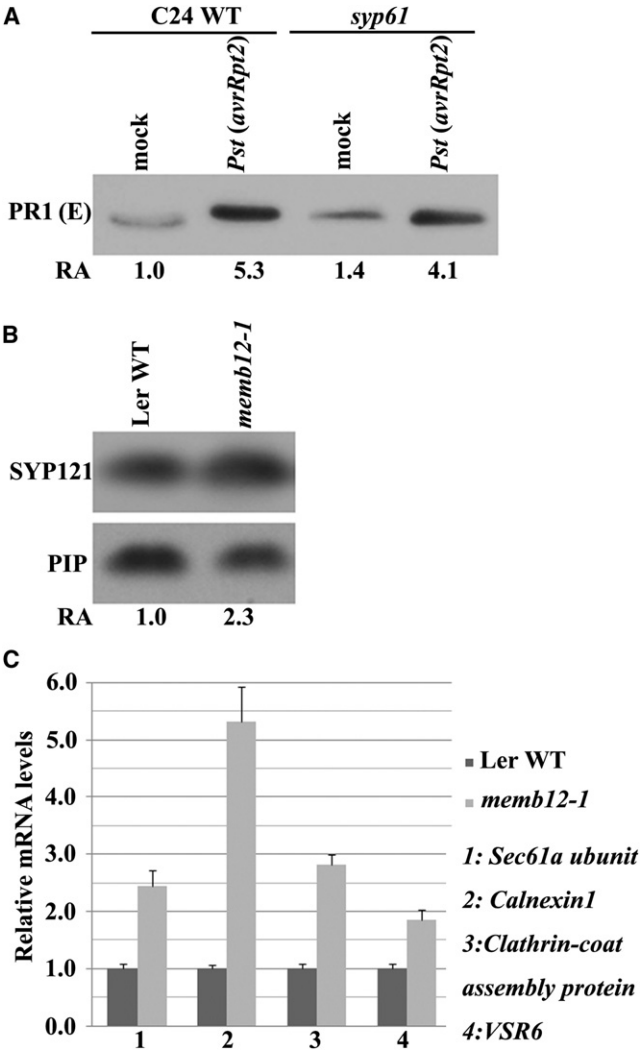

Figure 5. MEMB12 Is Likely to Regulate Secretion of PR Proteins in a Rather Specific Manner

(A) Mutation of another intracellular SNARE gene *SYP61* does not interfere with PR1 secretion. Secreted proteins were isolated from *syp61* and the corresponding C24 WT and detected as in Figure 4B. Experiments were performed two times with similar results.

(B) MEMB12 has weak effect on secretion of a PM-localized SNARE protein, SYP121. PM proteins were fractionated from 4-week-old mock- and *Pst* (*avrRpt2*)-treated tissue collected at 12 hpi. SYP121 was detected by SYP121 antibody (Collins et al., 2003). PIP-28RD (AT2G37180) was used as a loading control. Similar results were obtained from three biological repeats.

(C) Genes involved in protein folding and secretory pathways were coordinately upregulated in *memb12-1*. The transcript levels of some reported secretory-related genes (Wang et al., 2005) were detected by real-time RT-PCR. Expression levels in Ler WT plants were assigned as 1.0. Error bars indicate standard deviation from three technical repeats. Similar results were obtained in two biological replicates. See Table S3 for detailed primer and probe sequences.

together, our results suggest that miR393b* contributes to AGO2-regulated innate immunity by suppressing *MEMB12* and subsequently promoting effective secretion of antimicrobial PR proteins.

miR393b* Overexpression Plants Resemble *memb12* Mutant in Disease Resistance Responses

To determine whether overexpression of miR393b* results in a phenotype similar to the loss-of-function mutant of its target, *MEMB12*, we generated transgenic plants overexpressing the *MIR393b* gene controlled by the constitutive *CaMV* 35S promoter and selected the lines that expressed high level of miR393b* for bacterial growth assay and PR1 secretion analysis (Figure S4A). These plants showed enhanced disease resistance to *Pst* (*avrRpt2*) (Figure 6A) as well as increased PR1 protein accumulation and secretion (Figure 6B), which nicely resembled the phenotype of *memb12-1* in resistance responses (Figure 4). However, in these *MIR393b* overexpression plants, miR393 was also produced from the same *MIR393b* precursor (Figure S4A), which was evidenced by the curly leaf phenotype that is reminiscent of the double and triple mutants of the miR393 targets: *tir1/afb2* and *tir1/afb2/afb3* (Figures 6C, 5I, and 5J in Dharmasiri et al., 2005). Plants overexpressing *MIR393a* show enhanced resistance to virulent strain *Pst* DC3000 but have no obvious effect on *Pst* (*avrRpt2*)-triggered ETI (Navarro et al., 2006). Because *MIR393a* and *MIR393b* give rise to the same miR393, the positive regulatory effect of *MIR393b* on *Pst* (*avrRpt2*)-triggered ETI is due to the generation of miR393b*. However, it is impossible to tell whether the increased secretion of PR1 is due to the overexpression of miR393b* or miR393 in our *MIR393b* overexpression lines.

To distinguish the effects of miR393b* from that of miR393 on PR1 secretion, we used Web MicroRNA Designer and made an artificial miR393b* (amiR393b*) construct that produced miR393b* and the reverse complementary strand of miR393b* (referred to as miR393b**), which contains five different nucleotides from miR393 sequences (Figure 6D) (Schwab et al., 2006). The amiR393b* transgenic plants with high expression level of miR393b* were selected and no longer displayed the phenotype of altered auxin signaling (Figures 6C and S4B). Thus, we succeeded in uncoupling the effect of miR393b* and miR393 in these plants. We still observed increased PR1 secretion in these transgenic lines expressing artificial miR393b* (Figure 6E), which resembled the phenotype of *memb12*. These results support that *MEMB12* is indeed one of the major targets of miR393b* and regulates PR1 secretion.

DISCUSSION

miRNA* was once considered as a useless by-product of miRNA biogenesis (Jones-Rhoades et al., 2006; Schwarz et al., 2003). Here, we identified a functional miRNA* that regulates plant immunity along with its cognate miRNA partner. Thus, miRNA genes have the potential to generate more than one functional sRNA under certain conditions. miRNA393* and miRNA393 represent an example of a pair of miRNA* and miRNA that function through different AGOs in vivo and regulate two different cellular pathways in innate immunity. miR393* is loaded into AGO2, targets genes involved in protein trafficking, and regulates plant immune responses, mainly ETI, by promoting exocytosis of PR proteins; miR393 is loaded into AGO1 and contributes to PTI by targeting auxin receptors and suppressing the auxin signaling pathway.

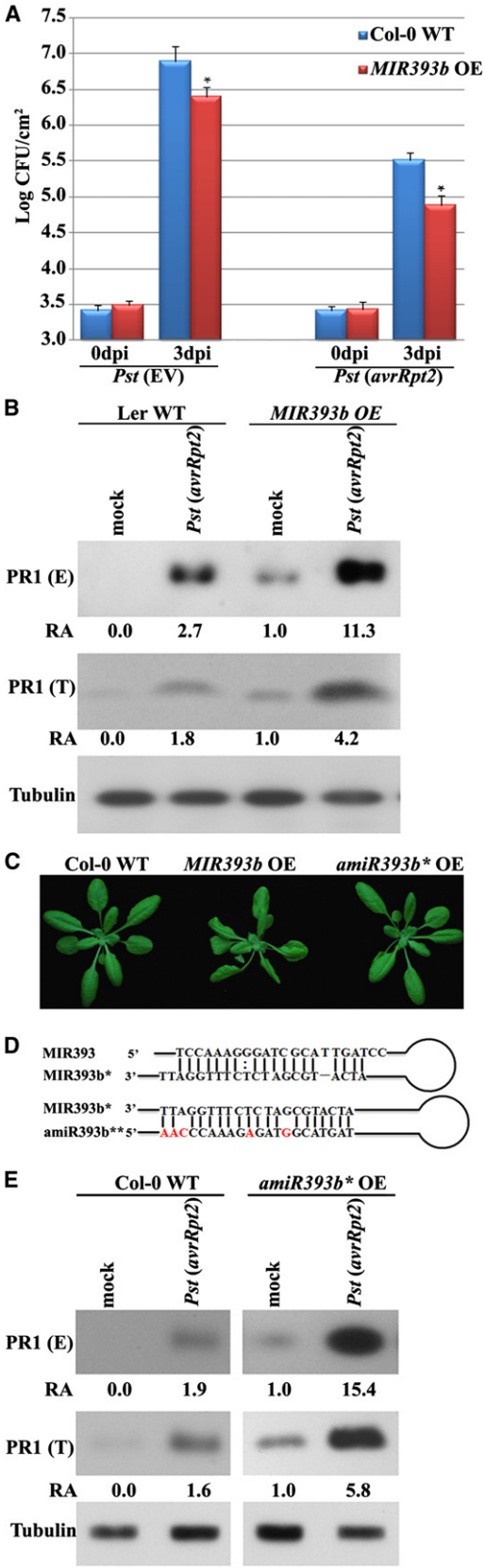

Figure 6. Overexpression of miR393b* Resembles *memb12-1* in Disease Resistance Responses

(A) *MIR393b* overexpression plants (*MIR393b* OE) were more susceptible to both *Pst* (EV) and *Pst* (*avrRpt2*) than WT plants. Pathogen growth was measured as in Figure 1C. Error bars represent standard deviation of six leaf discs (*$p < 0.05$). Similar results were obtained from three biological replicates.

(B) Overexpression of *MIR393b* promotes PR1 secretion. The level of PR1 was measured as in Figure 4B. Three biological repeats yielded similar results.

(C) Developmental phenotypes of transgenic plants overexpressing *MIR393b* (middle) and amiR393b* (amiR393b* OE, right). Pictures were taken from 3-week-old plants.

(D) Sequences of miR393/393b* and miR393b*/393b** for generating transgenic *MIR393b* and amiR393b* plants. The nucleotides that are different between miR393 and miR393b** are in red.

(E) amiR393b* transgenic plants show enhanced PR1 secretion. Experiments were repeated twice with similar results. See Figure S4 for the characterization of *MIR393b* and amiR393b* transgenic plants.

Strand selection of miRNA/miRNA* duplex within AGO complexes is largely determined by asymmetrical thermodynamic stability of the duplex termini (Khvorova et al., 2003; Schwarz et al., 2003). The strand with less stability at its 5′ terminus is incorporated as the guide strand (miRNA), while the other strand (so-called passenger strand or miRNA*) is mostly degraded. However, here we show that different AGO proteins select different guide strands within the same miRNA/miRNA* duplex regardless of their thermodynamic stability. sRNA loading into AGOs in plants is known to conform to the "5′ first nucleotide recognition" model (Mi et al., 2008; Montgomery et al., 2008), in which different AGOs preferentially associate with sRNAs with distinct 5′ first nucleotides. For example, AGO1 prefers uridine (U), AGO2 and AGO4 prefer adenosine (A), and AGO5 prefers cytosine (C). The fact that miR393 and miR393* start with 5′-terminal U and A, respectively, fits this model well. However, the other miRNA*s that were highly enriched in AGO2-IP fraction do not have 5′-terminal A (Table 1), such as miR165a* and miR396b*, which have 5′-terminal G. On the contrary, miR390, which features a 5′-terminal A, binds predominantly to AGO7 but not AGO2 (Montgomery et al., 2008). Thus, there must be other factors that help determine sRNA loading. Although all *Arabidopsis* AGO proteins contain the three conserved functional PAZ, MID, and PIWI domains, they have very different N-terminal regions. Even within the conserved domains, there are marked differences. For example, AGO2 and AGO3 are the only *Arabidopsis* AGOs that contain an Asp-Asp-Asp (DDD) motif instead of the conventional Asp-Asp-His (DDH) motif within the PIWI domain. This DDD motif is similar to that in bacterial RNaseH enzymes with cleavage activity (Nowotny et al., 2005; Vaucheret, 2008). It is likely that these sequence differences among AGO proteins may allow their interactions with different cofactors and direct distinct sRNA loading. The finding that the double-stranded RNA-binding protein DRB1 assists AGO1 loading of some miRNAs supports the idea that additional components are required for determination of sRNA binding (Eamens et al., 2009).

Protein secretory systems appear to play an important role in plant defense (Bednarek et al., 2010; Collins et al., 2003; Kalde et al., 2007; Kwon et al., 2008; Nomura et al., 2006). The SNARE proteins that have been identified to be involved in immune

responses are mostly associated with the PM (Bednarek et al., 2010; Collins et al., 2003; Kalde et al., 2007; Kwon et al., 2008). Here, we identified a previously uncharacterized intracellular SNARE, MEMB12, as a miR393b* target. Upon bacterial infection, suppression of MEMB12 by miR393b* promotes the secretion and accumulation of PR1 protein and contributes to resistance. MEMB12 is mainly localized to the Golgi and mediates protein trafficking between the Golgi and the ER (Uemura et al., 2004). Our results suggest that MEMB12 may be responsible for the retrograde trafficking from the Golgi to the ER for protein recycling and balance maintenance. MEMB12 and its close homolog MEMB11 are homologous to Bos1 in yeast and GS27 or membrin in mammals and regulate retrograde protein transport between Golgi and endoplasmic reticulum (ER) (Bubeck et al., 2008; Chatre et al., 2005), which is consistent with our results that downregulation of MEMB12 promotes PR1 secretion, likely through inhibiting retrograde transport and protein recycling. Mutation in another intracellular SNARE protein, SYP61, had no effect on the secretion of PR1, indicating that not all the SNARE proteins affect secretion of PR proteins. Mutation in MEMB12 has a weak effect on the secretion of the PM-associated syntaxin SYP121, suggesting that different SNARE proteins may be responsible for transporting different sets of proteins. This specificity is also observed in other SNAREs. For example, VTI12 but not its close homolog VTI11 affects the transport of storage proteins (Sanmartín et al., 2007). These results suggest the specialization of MEMB12 in controlling the secretion of PR proteins for immune responses. In addition to targeting MEMB12, miR393b* was predicted to target two other proteins involved in trafficking, VPS54 and EXO70H3. Like MEMB12, VPS54 is also Golgi localized and involved in the retrograde trafficking (Conibear and Stevens, 2000; Guermonprez et al., 2008). These results suggest that the immunity-specific secretory pathway is under regulation and fine-tuning by sRNA-mediated RNAi in response to pathogen attacks.

Our work suggests that *Arabidopsis* employs AGO2 as an important RNAi effector in plant antibacterial immunity. AGO2 also contributes to antiviral defenses against two viruses carrying silencing suppressors that target AGO1 (Harvey et al., 2011). Repression of AGO1 by viral suppressors leads to the downregulation of miR403 and subsequent induction of AGO2. It is unlikely that AGO2 induction by *Pst* is due to the same mechanism because strong induction of AGO2 by bacterial infection was still observed in *ago1-27* mutant (Figure S1H). Furthermore, we did not observe any suppression of miR403 by these bacterial strains (Figure S1I). miR403 targets both AGO2 and AGO3 at their 3′ UTR, but only AGO2 was induced by *Pst*. We believe that induction of AGO2 by bacteria may mainly occur at the transcriptional level and is mechanistically different from the induction triggered by viruses. Several defense responsive *cis*-elements, including the W-box motif, elicitor-responsive element, and gibberellin-responsive element, are present in the *AGO2* promoter, and future studies will elucidate their functions in *AGO2* induction upon bacteria challenges.

AGO2 associates with a large array of sRNAs, among which miR393b* is one of the most abundant. It would be interesting to test whether other AGO2-associated sRNAs and their targets are also involved in plant immunity. We speculate that AGO2 may regulate and coordinate the expression of a group of genes involved in various pathways of plant immunity by binding to a group of functional sRNAs.

EXPERIMENTAL PROCEDURES

Bacterial Infection

Bacterial growth assay and HR assay were performed as described (Katiyar-Agarwal et al., 2006, 2007). For RNA extraction and the HR assay, plants were inoculated with *Pst* strains at a concentration of 1×10^7 cfu/ml. For the bacterial growth assay, 5×10^5 cfu/ml was used. At least six leaf discs were collected for each experiment. Student's t test was employed to determine the significant difference between mutants and control plants.

Generation of Transgenic Plants

To generate the *AGO3*-RNAi construct, the 1–464 nt fragment of *AGO3* coding sequence was amplified and cloned into pJawohl8-RNAi (EMBO database ID AF408413). The construct was transformed into *ago2* and *ago2ago7* to generate *ago2ago3* and *ago2ago3ago7* mutants, respectively. Transgenic *35S::YFP:MEMB12-wt* or *35S::YFP:MEMB12-mu* plants were generated by transformation of binary construct pEG104 carrying the WT full-length *MEMB12* CDS or the mutated version with six altered nucleotides in the miR393b* target site (Earley et al., 2006). Overexpression constructs of *miR393b* and *amiR393b** were generated by cloning the miR393b precursor or artificial miRNA precursor using miR319 backbone (based on Web MicroRNA Designer) into a Gateway destination vector, pEG100 (Earley et al., 2006; Schwab et al., 2006). Primer sequences are listed in Table S3.

Cloning of AGO-Associated sRNAs and sRNA Library Construction

Mock- or *Pst* (*avrRpt2*)-treated *AGO2::3HA-AGO2 Arabidopsis* plants were used for AGO1- and AGO2-IP at 12 hpi. Coimmunoprecipitation and sRNA purification were performed as described by Mi et al. (2008). To avoid saturation, we used an excessive amount of protein A beads (Roche) and antibodies for the pull-down, about 50 μl of protein A beads for the extracts from 0.15 g plant tissue. For sRNA library construction, the miRCat sRNA cloning linkers were used, and manufacturer's protocol was followed (miRCat sRNA cloning kit; IDT). *MEMB12* transcript was detected by nested RT-PCR from AGO2-associated RNAs.

Protein Extraction and Analysis

The intercellular wash fluid was collected from the same amount of tissue by centrifuging the leaves at 1500 *g* for 5 min as described previously (Wang et al., 2005). The proteins from the same volume of intercellular fluid for each sample were analyzed by western blot analysis. Total proteins were examined by western blot analysis using α-tubulin as a loading control and RA measurement. For PM protein extraction, the PM fraction was isolated with a Dextran-PEG3500 two-phase system (Santoni, 2007). PM-associated PIP was used as a control.

Identification of Target Genes of miRNA*s

To identify miRNA* target genes, we followed the guideline for target prediction (Allen et al., 2005) with several modifications. Only one gap located in the sRNA was allowed, but with double penalty. Nucleotides at positions 10 and 11 of the sRNA must be a perfect match with its target. A maximum of three continuous mismatches was allowed if the mismatch region contained at least two G:U pairs and the penalty score of the region was multiplied by 1.5. We used ≤ 5.5 as the cutoff score for selecting the miRNA* targets.

ACCESSION NUMBERS

We used Illumina deep sequencing to analyze the AGO1- and AGO2-associated sRNA population after *Pst* (*avrRpt2*) and mock treatments. The data set was deposited into NCBI (GSE26161).

SUPPLEMENTAL INFORMATION

Supplemental Information includes Supplemental Experimental Procedures, Supplemental References, four figures, and three tables and can be found with this article online at doi:10.1016/j.molcel.2011.04.010.

ACKNOWLEDGMENTS

We thank Xinnian Dong, Jian-Kang Zhu, Thomas Eulgem, Isgouhi Kaloshian, Federica Brandizzi, Yifan Lii, and Arne Weiberg for helpful comments and Dongdong Niu for experimental assistance. We thank Xinnian Dong, David Baulcombe, Paul Schulze-Lefert, and Yijun Qi for providing antibodies; Jim Carrington for providing the AGO2::3HA-AGO2 line and mutant seeds; and David Baulcombe, John Clarke, and Herve Vaucheret for providing mutant seeds. This work was supported by the NIH (R01 GM093008), an NSF Career Award (MCB-0642843), and an AES-CE Research Allocation Award (PPA-7517H) to H.J.

Received: January 18, 2011
Revised: March 10, 2011
Accepted: April 20, 2011
Published: May 5, 2011

REFERENCES

Agorio, A., and Vera, P. (2007). ARGONAUTE4 is required for resistance to Pseudomonas syringae in Arabidopsis. Plant Cell *19*, 3778–3790.

Allen, E., Xie, Z., Gustafson, A.M., and Carrington, J.C. (2005). microRNA-directed phasing during trans-acting siRNA biogenesis in plants. Cell *121*, 207–221.

Bednarek, P., Kwon, C., and Schulze-Lefert, P. (2010). Not a peripheral issue: secretion in plant-microbe interactions. Curr. Opin. Plant Biol. *13*, 378–387.

Bubeck, J., Scheuring, D., Hummel, E., Langhans, M., Viotti, C., Foresti, O., Denecke, J., Banfield, D.K., and Robinson, D.G. (2008). The syntaxins SYP31 and SYP81 control ER-Golgi trafficking in the plant secretory pathway. Traffic *9*, 1629–1652.

Chatre, L., Brandizzi, F., Hocquellet, A., Hawes, C., and Moreau, P. (2005). Sec22 and Memb11 are v-SNAREs of the anterograde endoplasmic reticulum-Golgi pathway in tobacco leaf epidermal cells. Plant Physiol. *139*, 1244–1254.

Chellappan, P., Xia, J., Zhou, X., Gao, S., Zhang, X., Coutino, G., Vazquez, F., Zhang, W., and Jin, H. (2010). siRNAs from miRNA sites mediate DNA methylation of target genes. Nucleic Acids Res. *38*, 6883–6894.

Chisholm, S.T., Coaker, G., Day, B., and Staskawicz, B.J. (2006). Host-microbe interactions: shaping the evolution of the plant immune response. Cell *124*, 803–814.

Collins, N.C., Thordal-Christensen, H., Lipka, V., Bau, S., Kombrink, E., Qiu, J.L., Hückelhoven, R., Stein, M., Freialdenhoven, A., Somerville, S.C., and Schulze-Lefert, P. (2003). SNARE-protein-mediated disease resistance at the plant cell wall. Nature *425*, 973–977.

Conibear, E., and Stevens, T.H. (2000). Vps52p, Vps53p, and Vps54p form a novel multisubunit complex required for protein sorting at the yeast late Golgi. Mol. Biol. Cell *11*, 305–323.

Dharmasiri, N., Dharmasiri, S., Weijers, D., Lechner, E., Yamada, M., Hobbie, L., Ehrismann, J.S., Jürgens, G., and Estelle, M. (2005). Plant development is regulated by a family of auxin receptor F box proteins. Dev. Cell *9*, 109–119.

Ding, S.W. (2010). RNA-based antiviral immunity. Nat. Rev. Immunol. *10*, 632–644.

Eamens, A.L., Smith, N.A., Curtin, S.J., Wang, M.B., and Waterhouse, P.M. (2009). The Arabidopsis thaliana double-stranded RNA binding protein DRB1 directs guide strand selection from microRNA duplexes. RNA *15*, 2219–2235.

Earley, K.W., Haag, J.R., Pontes, O., Opper, K., Juehne, T., Song, K.M., and Pikaard, C.S. (2006). Gateway-compatible vectors for plant functional genomics and proteomics. Plant J. *45*, 616–629.

Geldner, N., Dénervaud-Tendon, V., Hyman, D.L., Mayer, U., Stierhof, Y.D., and Chory, J. (2009). Rapid, combinatorial analysis of membrane compartments in intact plants with a multicolor marker set. Plant J. *59*, 169–178.

Ghildiyal, M., Xu, J., Seitz, H., Weng, Z., and Zamore, P.D. (2010). Sorting of Drosophila small silencing RNAs partitions microRNA* strands into the RNA interference pathway. RNA *16*, 43–56.

Guermonprez, H., Smertenko, A., Crosnier, M.T., Durandet, M., Vrielynck, N., Guerche, P., Hussey, P.J., Satiat-Jeunemaitre, B., and Bonhomme, S. (2008). The POK/AtVPS52 protein localizes to several distinct post-Golgi compartments in sporophytic and gametophytic cells. J. Exp. Bot. *59*, 3087–3098.

Guo, L., and Lu, Z. (2010). The fate of miRNA* strand through evolutionary analysis: implication for degradation as merely carrier strand or potential regulatory molecule? PLoS ONE *5*, e11387.

Harvey, J.J., Lewsey, M.G., Patel, K., Westwood, J., Heimstädt, S., Carr, J.P., and Baulcombe, D.C. (2011). An antiviral defense role of AGO2 in plants. PLoS ONE *6*, e14639.

Havecker, E.R., Wallbridge, L.M., Hardcastle, T.J., Bush, M.S., Kelly, K.A., Dunn, R.M., Schwach, F., Doonan, J.H., and Baulcombe, D.C. (2010). The Arabidopsis RNA-directed DNA methylation argonautes functionally diverge based on their expression and interaction with target loci. Plant Cell *22*, 321–334.

Hunter, C., Sun, H., and Poethig, R.S. (2003). The Arabidopsis heterochronic gene ZIPPY is an ARGONAUTE family member. Curr. Biol. *13*, 1734–1739.

Hutvagner, G., and Simard, M.J. (2008). Argonaute proteins: key players in RNA silencing. Nat. Rev. Mol. Cell Biol. *9*, 22–32.

Jones, J.D.G., and Dangl, J.L. (2006). The plant immune system. Nature *444*, 323–329.

Jones-Rhoades, M.W., Bartel, D.P., and Bartel, B. (2006). MicroRNAS and their regulatory roles in plants. Annu. Rev. Plant Biol. *57*, 19–53.

Kalde, M., Nühse, T.S., Findlay, K., and Peck, S.C. (2007). The syntaxin SYP132 contributes to plant resistance against bacteria and secretion of pathogenesis-related protein 1. Proc. Natl. Acad. Sci. USA *104*, 11850–11855.

Katiyar-Agarwal, S., Morgan, R., Dahlbeck, D., Borsani, O., Villegas, A., Jr., Zhu, J.K., Staskawicz, B.J., and Jin, H. (2006). A pathogen-inducible endogenous siRNA in plant immunity. Proc. Natl. Acad. Sci. USA *103*, 18002–18007.

Katiyar-Agarwal, S., Gao, S., Vivian-Smith, A., and Jin, H. (2007). A novel class of bacteria-induced small RNAs in Arabidopsis. Genes Dev. *21*, 3123–3134.

Khvorova, A., Reynolds, A., and Jayasena, S.D. (2003). Functional siRNAs and miRNAs exhibit strand bias. Cell *115*, 209–216.

Kwon, C., Neu, C., Pajonk, S., Yun, H.S., Lipka, U., Humphry, M., Bau, S., Straus, M., Kwaaitaal, M., Rampelt, H., et al. (2008). Co-option of a default secretory pathway for plant immune responses. Nature *451*, 835–840.

Li, S., van Os, G.M., Ren, S., Yu, D., Ketelaar, T., Emons, A.M., and Liu, C.M. (2010a). Expression and functional analyses of EXO70 genes in Arabidopsis implicate their roles in regulating cell type-specific exocytosis. Plant Physiol. *154*, 1819–1830.

Li, Y., Zhang, Q., Zhang, J., Wu, L., Qi, Y., and Zhou, J.M. (2010b). Identification of microRNAs involved in pathogen-associated molecular pattern-triggered plant innate immunity. Plant Physiol. *152*, 2222–2231.

Lobbes, D., Rallapalli, G., Schmidt, D.D., Martin, C., and Clarke, J. (2006). SERRATE: a new player on the plant microRNA scene. EMBO Rep. *7*, 1052–1058.

Mallory, A., and Vaucheret, H. (2010). Form, function, and regulation of ARGONAUTE proteins. Plant Cell *22*, 3879–3889.

Matheson, L.A., Hanton, S.L., and Brandizzi, F. (2006). Traffic between the plant endoplasmic reticulum and Golgi apparatus: to the Golgi and beyond. Curr. Opin. Plant Biol. *9*, 601–609.

Mi, S.J., Cai, T., Hu, Y.G., Chen, Y., Hodges, E., Ni, F.R., Wu, L., Li, S., Zhou, H., Long, C.Z., et al. (2008). Sorting of small RNAs into Arabidopsis argonaute complexes is directed by the 5′ terminal nucleotide. Cell *133*, 116–127.

Montgomery, T.A., Howell, M.D., Cuperus, J.T., Li, D.W., Hansen, J.E., Alexander, A.L., Chapman, E.J., Fahlgren, N., Allen, E., and Carrington, J.C.

(2008). Specificity of ARGONAUTE7-miR390 interaction and dual functionality in TAS3 trans-acting siRNA formation. Cell *133*, 128–141.

Morel, J.B., Godon, C., Mourrain, P., Béclin, C., Boutet, S., Feuerbach, F., Proux, F., and Vaucheret, H. (2002). Fertile hypomorphic ARGONAUTE (ago1) mutants impaired in post-transcriptional gene silencing and virus resistance. Plant Cell *14*, 629–639.

Navarro, L., Dunoyer, P., Jay, F., Arnold, B., Dharmasiri, N., Estelle, M., Voinnet, O., and Jones, J.D.G. (2006). A plant miRNA contributes to antibacterial resistance by repressing auxin signaling. Science *312*, 436–439.

Nomura, K., Debroy, S., Lee, Y.H., Pumplin, N., Jones, J., and He, S.Y. (2006). A bacterial virulence protein suppresses host innate immunity to cause plant disease. Science *313*, 220–223.

Nowotny, M., Gaidamakov, S.A., Crouch, R.J., and Yang, W. (2005). Crystal structures of RNase H bound to an RNA/DNA hybrid: substrate specificity and metal-dependent catalysis. Cell *121*, 1005–1016.

Okamura, K., Phillips, M.D., Tyler, D.M., Duan, H., Chou, Y.T., and Lai, E.C. (2008). The regulatory activity of microRNA* species has substantial influence on microRNA and 3′ UTR evolution. Nat. Struct. Mol. Biol. *15*, 354–363.

Padmanabhan, C., Zhang, X., and Jin, H. (2009). Host small RNAs are big contributors to plant innate immunity. Curr. Opin. Plant Biol. *12*, 465–472.

Robert, S., Chary, S.N., Drakakaki, G., Li, S., Yang, Z., Raikhel, N.V., and Hicks, G.R. (2008). Endosidin1 defines a compartment involved in endocytosis of the brassinosteroid receptor BRI1 and the auxin transporters PIN2 and AUX1. Proc. Natl. Acad. Sci. USA *105*, 8464–8469.

Sanderfoot, A.A., Kovaleva, V., Bassham, D.C., and Raikhel, N.V. (2001). Interactions between syntaxins identify at least five SNARE complexes within the Golgi/prevacuolar system of the Arabidopsis cell. Mol. Biol. Cell *12*, 3733–3743.

Sanmartín, M., Ordóñez, A., Sohn, E.J., Robert, S., Sánchez-Serrano, J.J., Surpin, M.A., Raikhel, N.V., and Rojo, E. (2007). Divergent functions of VTI12 and VTI11 in trafficking to storage and lytic vacuoles in Arabidopsis. Proc. Natl. Acad. Sci. USA *104*, 3645–3650.

Santoni, V. (2007). Plant plasma membrane protein extraction and solubilization for proteomic analysis. Methods Mol. Biol. *355*, 93–109.

Schwab, R., Ossowski, S., Riester, M., Warthmann, N., and Weigel, D. (2006). Highly specific gene silencing by artificial microRNAs in Arabidopsis. Plant Cell *18*, 1121–1133.

Schwarz, D.S., Hutvágner, G., Du, T., Xu, Z.S., Aronin, N., and Zamore, P.D. (2003). Asymmetry in the assembly of the RNAi enzyme complex. Cell *115*, 199–208.

Springer, P.S., McCombie, W.R., Sundaresan, V., and Martienssen, R.A. (1995). Gene trap tagging of PROLIFERA, an essential MCM2-3-5-like gene in Arabidopsis. Science *268*, 877–880.

Uemura, T., Ueda, T., Ohniwa, R.L., Nakano, A., Takeyasu, K., and Sato, M.H. (2004). Systematic analysis of SNARE molecules in Arabidopsis: dissection of the post-Golgi network in plant cells. Cell Struct. Funct. *29*, 49–65.

Vaucheret, H. (2008). Plant ARGONAUTES. Trends Plant Sci. *13*, 350–358.

Wang, D., Weaver, N.D., Kesarwani, M., and Dong, X. (2005). Induction of protein secretory pathway is required for systemic acquired resistance. Science *308*, 1036–1040.

Wessner, B., Gryadunov-Masutti, L., Tschan, H., Bachl, N., and Roth, E. (2010). Is there a role for microRNAs in exercise immunology? A synopsis of current literature and future developments. Exerc. Immunol. Rev. *16*, 22–39.

Zhang, W., Gao, S., Zhou, X., Xia, J., Chellappan, P., Zhang, X., and Jin, H. (2010). Multiple distinct small RNAs originate from the same microRNA precursors. Genome Biol. *11*, R81.

Zhang, W., Gao, S., Zhou, X., Chellappan, P., Chen, Z., Zhou, X., Zhang, X., Fromuth, N., Coutino, G., Coffey, M., and Jin, H. (2011). Bacteria-responsive microRNAs regulate plant innate immunity by modulating plant hormone networks. Plant Mol. Biol. *75*, 93–105.

Zhu, J.H., Gong, Z.Z., Zhang, C.Q., Song, C.P., Damsz, B., Inan, G., Koiwa, H., Zhu, J.K., Hasegawa, P.M., and Bressan, R.A. (2002). OSM1/SYP61: a syntaxin protein in Arabidopsis controls abscisic acid-mediated and non-abscisic acid-mediated responses to abiotic stress. Plant Cell *14*, 3009–3028.

Zipfel, C., Robatzek, S., Navarro, L., Oakeley, E.J., Jones, J.D.G., Felix, G., and Boller, T. (2004). Bacterial disease resistance in Arabidopsis through flagellin perception. Nature *428*, 764–767.